# Behavior of Screen-Grid Insulated Concrete Forms (ICF) Reinforced Concrete Walls Under Seismic Loads

[Yosra H. El Maghraby, Ezzat Fahmy, Mohamed N. Abdel Mooty]

*Abstract*— The current research addresses Screen Grid Insulated Concrete Forms (ICF) Reinforced Concrete walls, an innovative system that combines structural strength and sustainability. The system however is still developing with relatively few researches and yet not acknowledged by several design codes. The aim of this work is to further evaluate the structural behavior of SGICF walls. Results of this research may lead to   and performed.

The test program consisted of six walls that were divided into two sets. The first set was tested under combined axial and lateral monotonic load and the second set was tested under combined axial and cyclic lateral load. Each set consisted of three walls; a wall without openings, one with a window opening and the other with a door opening. The configuration and reinforcement of the walls in the two sets were similar.

This part of the research aims at understanding the effect of seismic loading on SGICF walls. Accordingly, a cyclic loading experimental program was performed to simulate earthquake action. Results of the cyclic loading test program indicated the energy dissipation capacity of the tested walls as well as their stiffness degradation under this type of loading. The aim of the monotonic loading experimental program was to act as control specimens to evaluate the effect of cyclic loading.

The test showed the cracking pattern, lateral load resisting capacity, energy dissipation and stiffness degradation of the different walls under the two types of loading. These results may be very useful for the design of SGICF walls under seismic loads.

*Keywords—Screen Grid ICF, In-plane monotonic loading, In-plane cyclic loading, Grid size, Presence of openings.*

## I. Introduction

With today's awareness of energy conservation and the need for sustainable structures, innovative building materials and structural systems continue to develop. Such systems focus on reducing the heat and solar gain, thus reducing energy and costs needed to optimize cooling or heating in a building while maintaining the required strength and ductility. Lightweight aggregates (LWA) masonry blocks and expanded polystyrene (EPS) masonry blocks are examples of new building materials that have shown high efficiency in energy conservation while maintaining the required mechanical properties. Aerated lightweight-ferrocement sandwich panels and Insulating Concrete Forms (ICF) are other examples of the structural systems that are efficient in energy consumption.

Yosra H. El Maghraby
The British University in Egypt
El Shouk City, Egypt

Ezzat Fahmy
The American University in Cairo
New Cairo, Egypy

Mohamed N. Abdel Mooty
Department of Structural Engineering, Cairo University
Giza, Egypt

While Egypt and the Gulf countries have large areas of uninhabited deserts. The need for sustainable structures to develop these vast unutilized areas became significant. The growing awareness of environmental issues the last five decades drew attention to the insulating concrete forms (ICF) since it is a system that combines sustainability and strength.

ICFs in general are a fast-growing technology in the construction industry. ICFs are hollow blocks or panels made of Expanded Polystyrene (EPS) where the construction crew assembles them like Legos to create a wall. Steel reinforcement is fixed inside these blocks or panels, and then concrete is poured to fill the gap between the two layers of foam [1].

ICF systems are categorized based on two characteristics; the shape of the foam and the shape of the concrete after being poured. The current research focuses on the behavior of the reinforced concrete core. Therefore, it is imperative to define the different concrete core shapes.

The cavities inside the foam have various shapes and when concrete is poured in these ICF units it is shaped likewise forming the concrete core. There are three shapes for the concrete core; flat, grid and post and beam [3]. "Flat Wall" systems yield continuous uniform thickness of concrete like a conventional concrete wall. "Grid Wall" systems have cylindrical horizontal and vertical intersecting concrete cores that are equally spaced. There are two types of the grid system; the waffle grid which has a thin layer of concrete in between the intersecting concrete cores and the screen grid which has no concrete layer in between the intersecting cores. "Post and Beam" systems have widely and variably spaced horizontal and vertical concrete columns completely encapsulated in foam.

This part of the research focuses on the effect of cyclic loading on SG-ICF walls. An experimental program was designed for this purpose.

## II. Experimental Program

A total of six full scale SGICF wall specimens were tested under combined axial and lateral in-plane monotonic and cyclic loading. SG1, SW1 and SD1 were tested under in-plane monotonic loading and SG2, SW2 and SD2 were tested under in plane cyclic loading. Monotonic loading tests were to fulfill the purpose of observing the cyclic loading effect on the walls by comparing their results to the cyclic loading results. Although in real applications the EPS panels will remain as integrated part of the wall, they were removed and the concrete core strands were exposed before testing for better detection of the concrete cracking.

### A. Geometrical Properties and Composition of Specimens

The tested SGICF walls had different layouts as shown in Fig. 1. Wall dimensions were based on the dimensions given in the PCA report [2]. The overall wall dimensions without

the EPS panels were 2000mm in height, 1000mm in width and 150mm in thickness. The overall thickness of the walls including the EPS Panel was 400mm. Walls SG1 and SG2 had grid dimensions of 400x400mm and consisted of 4 horizontal standard cores, 2 horizontal end cores and 3 vertical standard cores. Standard cores were cylinders of 150mm diameter and end cores were half cylinders. SW1 and SW2 had grid dimension of 250x250mm and consisted of 4 horizontal standard cores, 2 horizontal end cores and 4 vertical standard cores. SD1 and SD2 had grid dimension of 250x250mm and consisted of 2 horizontal standard cores, 1 horizontal end cores and 4 vertical standard cores as shown in Fig. 1. SG1 and SG2 consisted of $1\phi12$ bar in each vertical and horizontal core strand. SW1, SW2, SD1 and SD2 consist of $1\phi8$ bar in each vertical and horizontal core strand.
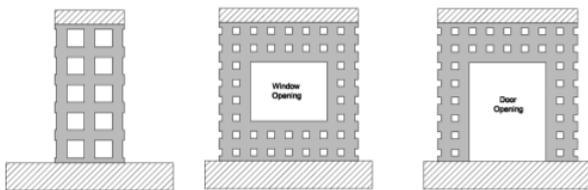


Figure 1 Concrete Core

The walls rested on a reinforced concrete foundation beam, with φ12mm dowels extended from the foundation beam for proper anchorage with the wall's vertical reinforcement. The steel bars of the vertical cores were extended 100mm above the wall for proper anchorage with the top concrete beam. The top concrete beam was provided to assure equal distribution the lateral load on the wall.

## B. *Test Setup and Instrumentation*

Fig. 2 shows the test setup. The vertical actuator for applying the vertical load was mounted on the steel testing rig while the horizontal actuator for applying the horizontal load was mounted on the lab's strong wall. The foundation beam of the wall assembly was attached to the strong floor using Z-shaped steel assembly as shown in Fig. 2. This supporting arrangement provided the required restraint against the horizontal movement in the direction of the lateral load and uplift from the floor. To achieve uniform vertical load distribution on the wall, the vertical actuator and load cell applied the vertical load on a steel beam supported on five steel rollers spaced equally along the length of the wall. Four steel C channels were fixed on the steel cross beams to restrict out of plane movement of the specimen.



**Figure 2 Test Setup**

Three LVDTs were placed; two of them to measure the vertical displacement due to uplift and one for the horizontal displacement at the top of the panel.

## C. *Test Procedure*

1. The foundation beam was cast first with the dowels in place. Then steel reinforcement was fixed at the designated locations. The foam formwork was then secured in place while ensuring the steel bars are centered in the foam cavities. The wall core together with their top beam were cast inside the EPS forms and were left to cure for a minimum of 28 days. Foam is then removed for visual observation of cracking pattern.

2. The wall was transported and placed at the testing rig and the foundation beam was fixed to the lab floor by the Z support. Vertical and horizontal actuators were fixed to the testing frame and lab strong wall respectively. The steel top beam and the steel rollers were placed on the top beam. Out of plane restraints were fixed in place. LVDTs and load cells were connected to the data logging system.

3. For the monotonic loading test, the vertical (axial) load was first applied then lateral load was applied and increased steadily in one direction till the peak load was reached and was then reduced to 80%. In many cases, the test was continued to complete failure. The test data were continuously recorded by a computerized data acquisition system and the load-displacement curve was also plotted on an analogue plotter.

4. For the cyclic loading test, reversed cyclic loading was achieved by pushing and pulling the specimen to a predetermined displacement (displacement-based test) to simulate earthquakes which generally imposes deformations on buildings that lead to the generation of straining actions in the members. Due to the complicated geometry and un-predictable behavior of the wall it was difficult to determine the early stages of deformation. Accordingly, the first set of cycles was set to a displacement of 2mm as the initial set then increased by a factor of 1.5 for each consecutive set of cycles. In the current test, the vertical (axial) load was first applied then the lateral displacement which was applied by pushing the specimen to a predetermined displacement, returned to its zero position, pulled to the same displacement then finally returned to its zero position. This is considered one cycle. Three cycles of the same displacement level took place then the test is stopped for inspection and marking of cracks.

## III.   Test Results

### A. *Specimen SG1*

SG1 is the wall specimen with a wide grid where the spacing between center to center of the vertical and horizontal core strands is 400 mm instead of 250 mm spacing in other specimens with openings. Fig. 3 illustrates the types of cracks in the wall; it shows that flexure and shear cracks developed after applying the lateral load and the wall finally failed in shear.

The illustrated cracking pattern in Fig. 3 indicates that the wall with wide grid spacing behaved more like a multi-story multi-bay frame rather than a shear wall. The positive moment, Fig. 3, at the connections between the columns (vertical strands) and the beams (horizontal strands) caused the developed cracks between these two elements as shown in Fig. 3. Also, the applied shear on the columns and beams of the frame (vertical and horizontal strands) resulted in the observed diagonal cracks. The diagonal cracks occurred in the vertical strand at level above the dowels since below this level the reinforcement is doubled due to the overlap between the dowels and the strands' reinforcing bars.

## B. *Specimen SG2*

Specimen SG2 withstood increased cyclic displacement up to 52mm, remaining intact with little damage. When the cyclic displacement value increased to 76 mm the vertical core on the left side completely collapsed as illustrated in Fig. 3. The load displacement curve in Fig. 4 shows the hysteresis loops through cyclic loading. The maximum load the specimen could withstand was 70.4 kN and the maximum displacement was 52mm.



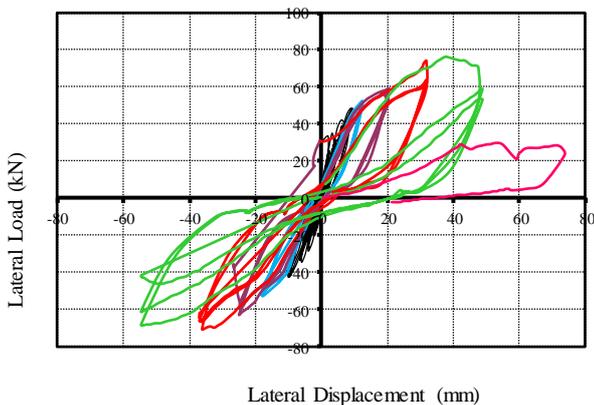**Figure 3 SG1 (left) and SG2 (right)**



**Figure 4 Load- displacement curve of SG2**

As stated earlier, reversed cyclic loading results in stiffness degradation and this is very clear when observing the load displacement curve of the first 3 cycles. Fig. 5 shows that stiffness of the specimen in the first half cycle was greater than the following cycles. This could be attributed to the minor cracks that were not visible and started to develop at the 2mm displacement level resulting in stiffness degradation.
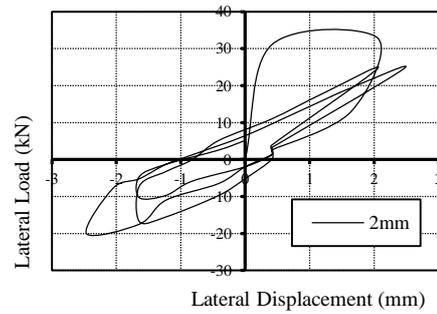


**Figure 5 First 3 cycles of SG2**

## C. *Specimen SW1*

Specimen SW1 had a window opening. The cracks initiated at the top right corners (the side of lateral load application) and at the bottom left corner of the window as shown in Fig. 6. Wall SW1 failed at lateral load of 89 kN due to shear without reaching the crushing strain of concrete. With the wide window opening, the specimen behaved more like a closed frame consisting of the part on top of the window, the two sides on the left and right of the window, and the part under the widow. The closed frame is supported along the entire wall width on the supporting foundation beam. Accordingly, at any load level the assumed frame would be subjected to axial, shear, and bending moment.



**Figure 4 Cracking of SW1, lower left corner (left), upper top corner (center), lower right corner (right)**

## D. *Specimen SW2*

Specimen SW2 withstood displacement up to 23 mm while standing intact. When the displacement value increased to 34 mm the vertical core on the left side completely collapsed as illustrated in Fig. 7 and the vertical steel bars buckled. During one of the cycles of displacement value 15mm the horizontal LVDT moved suddenly out of its position. The test was stopped, and the 3 cycles of displacement level 15 mm were repeated. For this reason, the load-displacement curve has discrepancies. The maximum load the specimen could take was 83.7 kN and the maximum displacement was 23mm.



**Figure 5 SW2 after cyclic loading**

Upon observing both Fig. 7 and Fig. 8 of the cracks and the load-displacement curve, it can be comprehended that up till the displacement level of 6.75 mm the wall was to a certain extent maintaining its strength and stiffness. Starting the displacement level of 10mm a drastic decrease in strength and stiffness occurred.
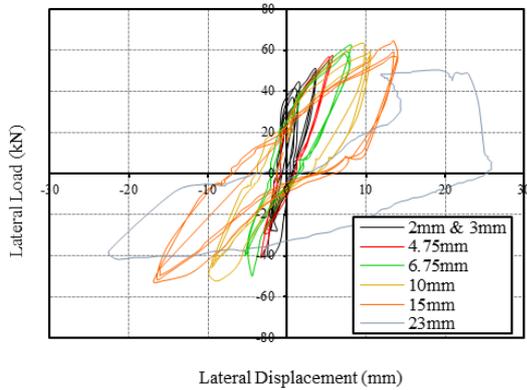


**Figure 6 Load- displacement curve of SW2**

### E. *Specimen SD1*

Specimen SD1 had a door opening. Like specimen SW1 the cracks initiated at the top right corner of the door. Cracks also developed later at the other corner of the door. A major crack was developed over the dowels of the wall at the right of the opening and then propagated diagonally. Diagonal cracks were also observed in the wall on the other side of the opening as shown in Fig. 9. Wall SD1 failed at lateral load of 90.4 kN due to diagonal shear without reaching the crushing strain of the concrete. This wall behaved more like a frame, like SW1, fixed at the foundation beam.



**Figure 7 SD1 after applying monotonic load**

### F. *Specimen SD2*

Specimen SD2 withstood displacement up to 15 mm, Fig. 10, while standing intact. When the displacement value increased to 23 mm the steel and the concrete of the vertical core strand on the left side completely collapsed as illustrated in Fig. 11 and the vertical steel bars buckled. The maximum load the specimen could take was 64.6 kN and the maximum displacement was 23mm.

When looking globally on the cracking pattern, it can be observed that the pattern is almost symmetric about the axis of symmetry of the wall and that the action of this wall with this size of opening is more like a frame with a grid beam and two grid columns.
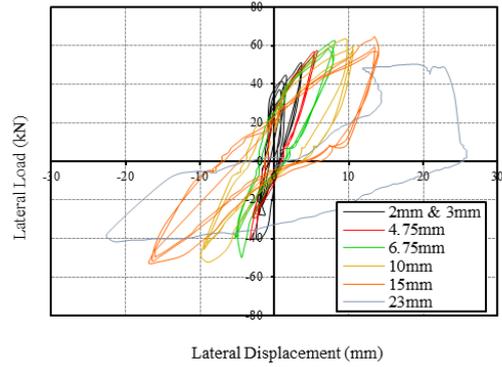


**Figure 10 Load- displacement curve of SD2**



**Figure 11 SD2 after applying cyclic load**

## IV. **Analysis**

### A. *Energy Dissipation*

One of the goals of performing cyclic load testing is to measure the capacity of the wall to dissipate energy during an earthquake event. Cyclic load testing yields a load-displacement curve in the form of hysteresis loops from which the energy dissipation capacity could be calculated. The area within the loops was calculated by numerical integration using the trapezoid method. Table 1 shows the values of energy dissipated by each specimen. It shows that SD2 dissipated energy less than SW2 by almost 23% which indicates the effect of the size of opening on the performance of the wall under seismic loading.

**Table 1 Energy Dissipation due to Cyclic Loading**

| Specimen | Max. Load (kN) | Max. Displacement (mm) | Energy Dissipated (kN.mm) |
|---|---|---|---|
| SG2 | 80 | 70 | 10,401.15 |
| SW2 | 80 | 30 | 11,004.70 |
| SD2 | 65 | 25 | 8,388.11 |

### B. *Stiffness Degradation*

Concrete members \undergo strength and stiffness degradation due to cracking during the reversed seismic loading. A measure of the percentage stiffness degradation of the 3 specimens is plotted in Fig. 12. SG2 is not comparable with SW2 and SD2 due to the different grid size as well as the different aspect ratio. However, when comparing SW2 to SD2, it shows that the degradation of SW2 is smoother than that of SD2. This indicates that the larger the opening the faster the wall loses its stiffness.
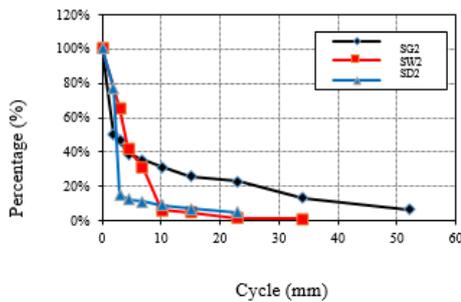
4

**Figure 8 Stiffness Degradation under Cyclic Loading**

## C. *Comparison of Monotonic and Cyclic Load Results*

Generally, the trend in Fig. 13 indicates that the two curves of the cyclic and monotonic loading start off having the same stiffness. Then, the curve of the monotonic loading loses its stiffness and the curve of the cyclic loading maintains its stiffness up to a higher load. This could be attributed to the fact that in monotonic loading the specimen is pushed, and cracks are formed and keep widening upon further pushing. This process makes the specimen less stiff. On the other hand, in the cyclic loading, the specimen is pushed, and a crack is created then the specimen is pulled back and closes the crack again. For this reason, the specimen maintains its stiffness up to a higher load. However, due to the reversed cycles of cracks opening and closing, the specimen deteriorates and fails at an earlier load accompanied with lower displacement.

Fig. 13 shows the load-displacement curve of specimens SG1, SW1, SD1 and the envelope of the load-displacement curve of SG2, SW2, and SD2. The figure shows that SG1 failed at almost 99 kN and SG2 failed at 74 kN which makes a difference of about 25%. The difference in the load carrying capacity of SW1 and SW2 was not large (88.8kN and 83.7kN for SW1 and SW2, respectively). The difference in the load carrying capacity of SD1 and SD2 was about 30%. By comparing the envelopes of SW2 and SD2, it could be concluded that the size of the opening significantly affects the load carrying capacity of the wall under cyclic loading which was not the case under monotonic loading.
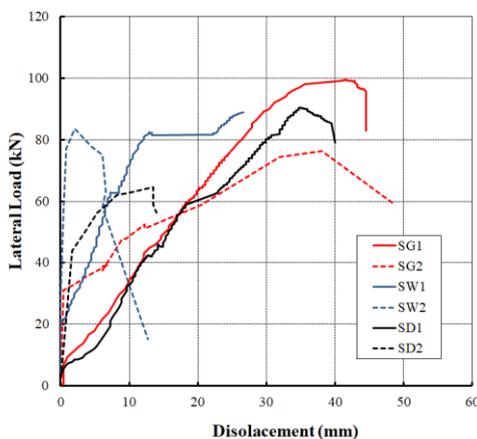


**Figure 9 Load-displacement curves for all test specimens**

## V. Conclusion

1. SGICF walls exhibit a stiffer behavior under in-plane cyclic loading than under in-plane monotonic loading. However, in cyclic loading due to the reversed cycles of cracks opening and closing, the wall deteriorates and fails at an earlier load accompanied with lower displacement.

2. The height of the opening in a SGICF wall significantly affected the lateral load carrying capacity of the wall under combined axial and in-plane cyclic loading unlike in combined axial and in-plane monotonic loading where the height of the opening did not affect the lateral load carrying capacity of the wall.

3. The energy dissipation capacity of a SGICF wall with window opening (SW2) is more than that of a SGICF wall with door opening of the same length (SD2) by almost 24% which indicates that the smaller the opening height the more a SGICF wall is able to dissipate energy.

4. The results also showed that the stiffness degradation of the wall with door opening (SD2) is more rapid than that of the wall with window opening of the same length (SW2).

### *Acknowledgment*

### *References*

[1] D. Benson, "The advantages of insulated concrete forms," New Hampshire Business Review, vol. 9, pp4.

[2] A. Mehrabi, "In-plane lateral load resistance of wall panels in residential buildings," PCA R&D Serial No. 2403 retrieved from the Portland Cement Association website http://www.cement.org/homes/data/sn2403.pdf

[3] P. A. Vanderf, S. J. Feige, P. Chammas and L. A. Leemay "Insulating concrete forms for residential design and construction," New York: McGraw Hill, 1997.